Deformation Behavior of AA8090/ TiO_2 Nanoparticulate Reinforced Metal Matrix Composites with Debonding Interfaces

[1]S. Sundara Rajan and A. Chennakesava Reddy[2]

[1]Scientist-F, Defence Research and Development Organisation, Hyderabad, India.
2Assistant Professor, Department of Mechanical Engineering, MJ College of Engineering and Technology, Hyderabad, India
dr_acreddy@yahoo.com

Abstract: A square array unit cell/ spherical particulate RVE models were employed to evaluate interfacial debonding using cohesive zone analysis. The particulate metal matrix composites are titanium oxide/AA8090 alloy at volume fractions of 10%, 20% and 30% TiO_2. Interface debonding was observed in all the composites. The stress concentration at interface delays the occurrence of interfacial debonding

Keywords: AA8090 alloy, titanium oxide, spherical particle, RVE model, finite element analysis, interface debonding.

1. INTRODUCTION

The use of filler particles as toughening agent in composites has received considerable attention in recent years. The macroscopic response of particle reinforced composites is influenced by not only the component properties and component concentrations, but also the interfacial interaction between the particles and the matrix. In particular, the inclusion of stiff particles to a soft matrix can lead to an increase in composite stiffness, strength, impact resistance, and abrasion resistance. In contrast to the numerous experimental investigations, there have been few theoretical investigations which consider the effect of interfacial debonding in the finite deformation regime [1-14].

This paper presents a computational framework capable of capturing the influence of interfacial debonding on the finite deformation response of particle reinforced composites. The present study considers the deformation of the interface between AA8090 alloy and TiO_2 nanoparticle. Representative volume elements (RVEs) models were taken from the periodic spherical particles in a square array distribution (figure 1).

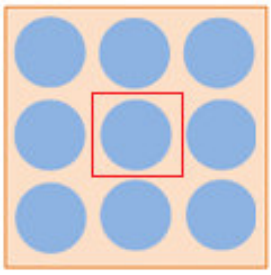

Figure 1: The RVE model.

2. MATERIALS AND METHODS

The computational framework considered in the present work is comprised of AA8090 alloy matrix material with an embedded spherical titanium oxide particle. The volume fractions of TiO_2 were 10%, 20%, and 30%. Initially, both AA8090 and TiO_2 were kept in contact with zero separation distance. PLANE183 element was used for the matrix and the nanoparticulates. The cohesive element is implemented as a linear element with four nodes. The finite element analysis was carried out for the single inclusion model undergoing a tensile load. The elastic material properties are given by $E_m = 77.0$ GPa, $E_p = 288$ GPa, $\nu_m = 0.33$ and $\nu_p = 0.29$.

Shear-log model is based on the assumption that all of the load transfer from matrix to particulate occurs via shear stresses acting on the particulate interface between the two constituents. The rate of change of the stress in the particulate to the interfacial shear stress at that point and the particulate radius, ‘r’ is given by:

$$\frac{d\sigma_p}{dx} = -\frac{2\tau_i}{r} \quad (1)$$

which may be regarded as the basic shear lag relationship.

The stress distribution in the particulate is determined by relating shear strains in the matrix around the particulate to the macroscopic strain of the composite. Some mathematical manipulation leads to a solution for the distribution of stress at a distance 'x' from the mid-point of the particulate which involves hyperbolic trig functions:

$$\sigma_p = E_p \varepsilon_c [1 - cosh(nx/r) sech(ns)] \quad (2)$$

where ε_c is the composite strain, s is the particulate aspect ratio (length/diameter) and n is a dimensionless constant given by:

$$n = \left[\frac{2E_m}{E_p(1+v_m)ln(1+v_p)}\right]^{1/2} \quad (3)$$

in which v_m is the Poisson ratio of the matrix. The variation of interfacial shear stress along the particulate length is derived, according to Equation (1), by differentiating this equation, to give:

$$\tau_i = \frac{n\varepsilon_c}{2} E_p sinh\left(\frac{nx}{r}\right) sech(ns) \quad (4)$$

The equation for the stress in the particulate, together with the assumption of a average tensile strain in the matrix equal to that imposed on the composite, can be used to evaluate the composite stiffness. This leads to:

$$\sigma_c = \varepsilon_c \left[v_p E_p \left(1 - \frac{tanh(ns)}{ns}\right) + (1 - v_p) E_m\right] \quad (5)$$

The expression in square brackets is the composite stiffness. The stiffness is a function of particulate aspect ratio, particulate/matrix stiffness ratio and particulate volume fraction.

If the particle deforms in an elastic manner (according to Hooke's law) then,

$$\tau = \frac{n}{2}\sigma_p \quad (6)$$

If interfacial debonding/yielding is considered to occur when the interfacial shear stress reaches its shear strength

$$\tau = \tau_{max} \quad (7)$$

For particle/matrix interfacial fracture can be established whereby,

$$\tau_{max} < \frac{n\sigma_p}{2} \quad (8)$$

This approach suggests that the outcome of a matrix crack impinging on an embedded particle depends on the balance between the particle strength and the shear strength of the interface. For plane strain conditions, the macro stress- macro strain relation is as follows:

$$\begin{Bmatrix} \overline{\sigma_x} \\ \overline{\sigma_y} \\ \overline{\tau_{xy}} \end{Bmatrix} = \begin{bmatrix} \overline{C_{11}} & \overline{C_{12}} & 0 \\ \overline{C_{21}} & \overline{C_{22}} & 0 \\ 0 & 0 & \overline{C_{33}} \end{bmatrix} \times \begin{Bmatrix} \overline{\varepsilon_x} \\ \overline{\varepsilon_y} \\ \overline{\gamma_{xy}} \end{Bmatrix} \quad (9)$$

The interfacial tractions can be obtained by transforming the micro stresses at the interface as given in Eq. (3):

$$t = \begin{Bmatrix} t_z \\ t_n \\ t_t \end{Bmatrix} = T\sigma \quad (10)$$

where, $T = \begin{bmatrix} 0 & 0 & 0 \\ cos^2\theta & sin^2\theta & 2sin\theta cos\theta \\ -sin\theta cos\theta & sin\theta cos\theta & cos^2\theta - sin^2\theta \end{bmatrix}$

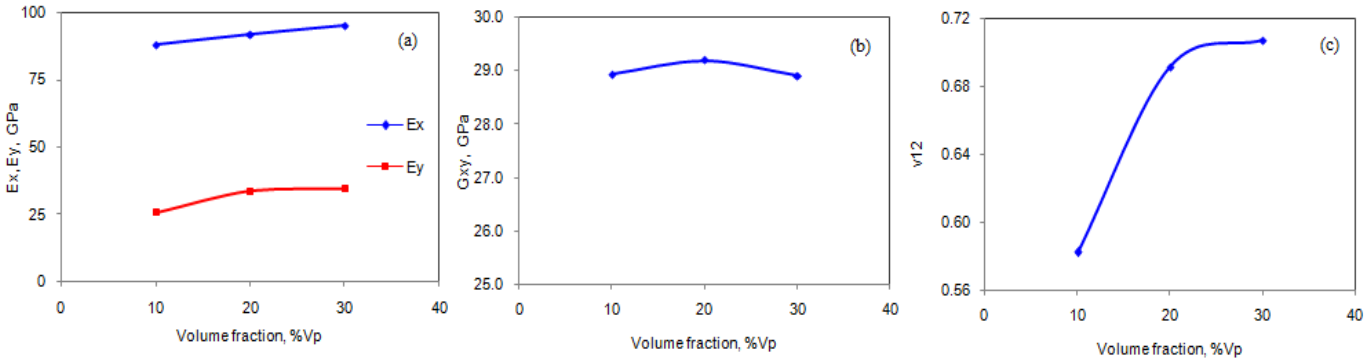

Figure 2: Effect of volume fraction on effective material properties.

3. RESULTS AND DISCUSSION

The tensile and compression moduli increased with volume fraction of TiO_2 as shown figure 2a. The shear modulus was nearly constant with increase in the volume fraction of TiO_2 in the composites (figure 2b). The major Poisson's ratio increased with volume fraction of TiO_2. The stiffness mismatch between TiO_2 nanoparticulate and AA8090 alloy matrix is 211 GPa. The condition $\tau_{max} < n\sigma_p/2$ is satisfied for the incidence of debonding in the composites including 10%, 20% and 30% TiO_2 (figure 3). The strain energy densities induced in the composites are shown in figure 4. It is observed that the strain energy density is in proportional to separation between the TiO_2 particle and AA8090 alloy matrix.

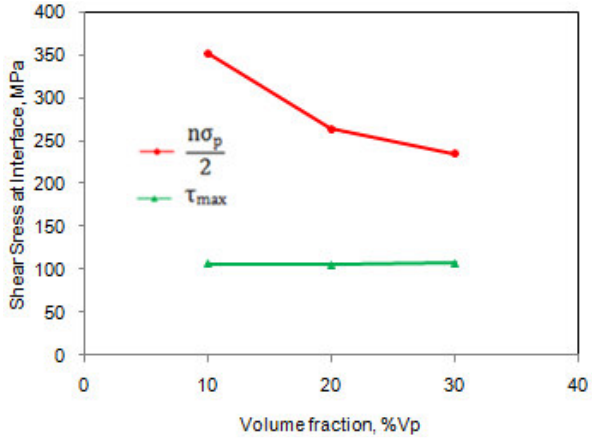

Figure 3: Fracture criteria of interface debonding.

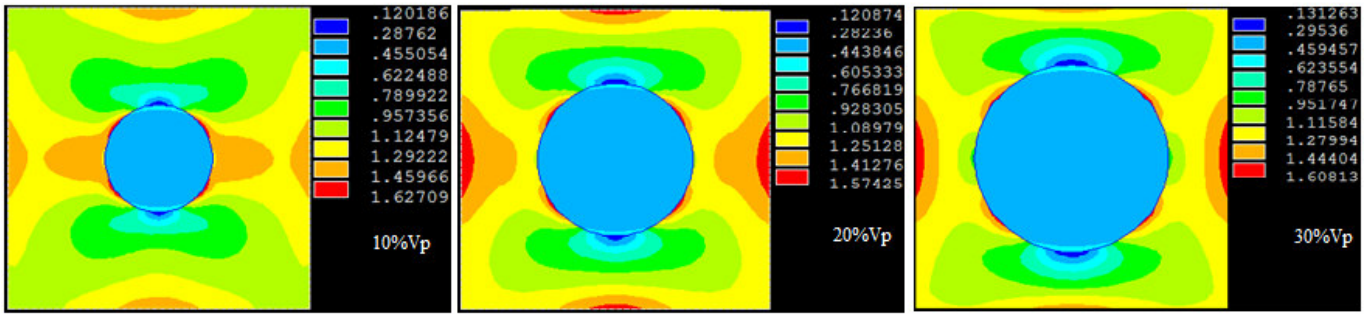

Figure 4: FEA results of strain energy densities.

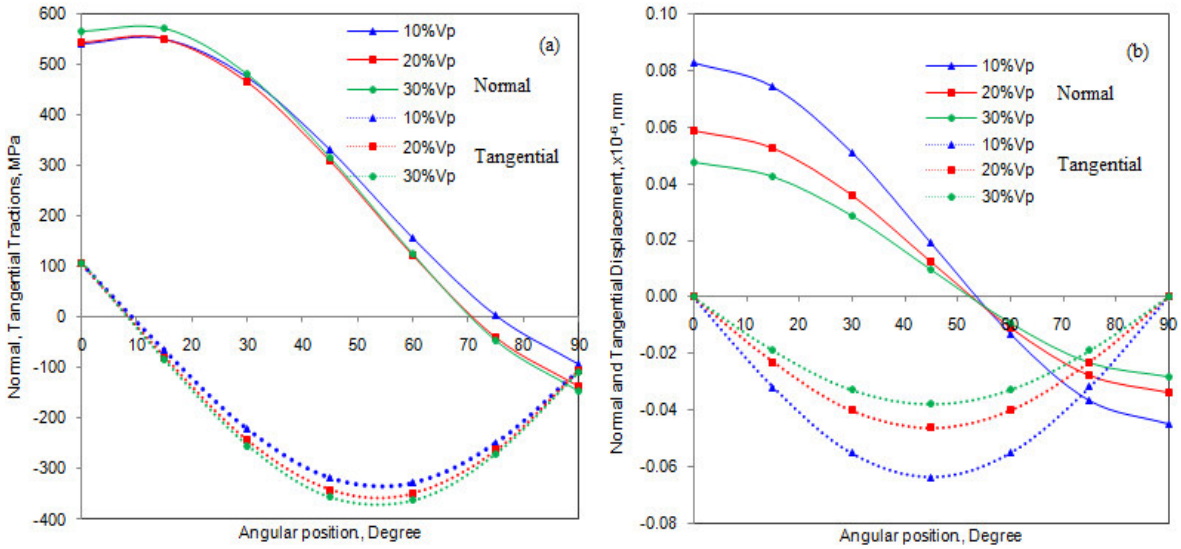

Figure 5: Normal and tangential: (a) tractions and (b) displacements.

The normal and tangential tractions are plotted in figure 5. Because of symmetry considerations, the variations of the interface stresses with circumferential location are plotted only for the range $0^o \leq \theta \leq 90^o$. The normal traction in the region of interface between TiO_2 nanoparticulate and AA8090 alloy matrix increased with increase of volume fraction of TiO_2. The plots shown are for the normal traction dominated failure. The maximum allowable normal separation of the cohesive element corresponds to the separation distance at which the traction decreases to near zero value.

4. CONCLUSION

The interface debonding occurred in the composites containing 10%, 20% and 30% volume fractions boron nitride. The stress concentration at interface, which delays the occurrence of interfacial debonding, increases the energy absorption capability.

REFERENCES

1. A. Chennakesava Reddy, Assessment of Debonding and Particulate Fracture Occurrences in Circular Silicon Nitride Particulate/AA5050 Alloy Metal Matrix Composites , National Conference on Materials and Manufacturing Processes, Hyderabad, India, 27-28 February1998, pp.104-109.
2. B. Kotiveera Chari and A. Chennakesava Reddy, Numerical Simulation of Particulate Fracture in Round Silicon Nitride Particulate/AA6061 Alloy Metal Matrix Composites, National Conference on Materials and Manufacturing Processes, Hyderabad, India, 27-28 February 1998, pp. 110-114.
3. H. B. Niranjan and A. Chennakesava Reddy, Effect of Elastic Moduli Mismatch on Particulate Fracture in AA7020/Silicon Nitride Particulate Metal Matrix Composites , National Conference on Materials and Manufacturing Processes, Hyderabad, India, 27-28 February, 1998, pp. 115-118,
4. P. Martin Jebaraj and A. Chennakesava Reddy, Cohesive Zone Modelling for Interface Debonding in AA8090/Silicon Nitride Nanoparticulate Metal Matrix Composites, National Conference on Materials and Manufacturing Processes, Hyderabad, India, 27-28 February 1998, pp. 119-122.
5. P. Martin Jebaraj and A. Chennakesava Reddy, Plane Strain Finite Element Modeling for Interface Debonding in AA1100/Silicon Oxide Nanoparticulate Metal Matrix Composites, National Conference on Materials and Manufacturing Processes, Hyderabad, India, 27-28 February 1998, pp. 123-126.
6. A. Chennakesava Reddy, Local Stress Differential for Particulate Fracture in AA2024/Titanium Carbide Nanoparticulate Metal Matrix Composites, National Conference on Materials and Manufacturing Processes, Hyderabad, India, 27-28 February 1998, pp. 127-131.
7. B. Kotiveera Chari and A. Chennakesava Reddy, Interface Debonding and Particulate Facture based on Strain Energy Density in AA3003/MgO Nanoparticulate Metal Matrix Composites, National Conference on Materials and Manufacturing Processes, Hyderabad, India, 27-28 February 1998, pp. 132-136.
8. H. B. Niranjan and A. Chennakesava Reddy, Numerical and Analytical Prediction of Interface Debonding in AA4015/Boron Nitride Nanoparticulate Metal Matrix Composites , National Conference on Materials and Manufacturing Processes, Hyderabad, India, 27-28 February 1998, pp. 137-140.
9. S. Sundara Rajan and A. Chennakesava Reddy, Effect of Particulate Volume Fraction on Particulate Cracking in AA5050/Zirconium Oxide Nanoparticulate Metal Matrix Composites , National Conference on Materials and Manufacturing Processes, Hyderabad, India, 27-28 February 1998, pp. 156-159.
10. S. Sundara Rajan and A. Chennakesava Reddy, Cohesive Zone Analysis for Interface Debonding in AA6061/Titanium Nitride Nanoparticulate Metal Matrix Composites , National Conference on Materials and Manufacturing Processes, Hyderabad, India, 27-28 February 1998, pp. 160-164.
11. A. Chennakesava Reddy, Effect of Particle Loading on Microealstic Behavior and interfacial Tractions of Boron Carbide/AA4015 Alloy Metal Matrix Composites, 1st International Conference on Composite Materials and Characterization, Bangalore, 14-15 march 1997, pp. 176-179.7
12. A. Chennakesava Reddy, Reckoning of Micro-stresses and interfacial Tractions in Titanium Boride/AA2024 Alloy Metal Matrix Composites, 1st International Conference on Composite Materials and Characterization, Bangalore, 14-15 march 1997, pp. 195-197.
13. A. Chennakesava Reddy, Interfacial Debonding Analysis in Terms of Interfacial Tractions for Titanium Boride/AA3003 Alloy Metal Matrix Composites, 1st National Conference on Modern Materials and Manufacturing , Pune, India, 19-20 December 1997, pp. 124-127.
14. A. Chennakesava Reddy, Evaluation of Debonding and Dislocation Occurrences in Rhombus Silicon Nitride Particulate/AA4015 Alloy Metal Matrix Composites, 1st National Conference on Modern Materials and Manufacturing , Pune, India, 19-20 December 1997, pp. 278-282.